

# The influence of tricuspid annuloplasty prostheses on ovine annular geometry and kinematics



Marcin Malinowski, MD,<sup>a,b</sup> Tomasz Jazwiec, MD,<sup>a,c</sup> Nathan Quay, BS,<sup>a</sup> Matthew Goehler, BS,<sup>a</sup> Manuel K. Rausch, PhD,<sup>d</sup> and Tomasz A. Timek, MD, PhD<sup>a</sup>

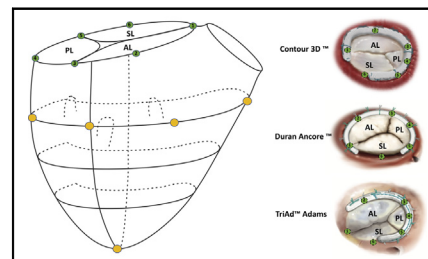
## ABSTRACT

**Background:** Surgical repair of functional tricuspid regurgitation is centered on annular reduction with artificial rings; however, the precise effect of prosthesis implantation on annular geometry, dynamics, and strain is unknown.

**Methods:** Forty healthy sheep had sonomicrometry crystals implanted around the tricuspid annulus and onto right ventricle free wall. Ten animals underwent tricuspid annuloplasty with a flexible Duran AnCore ring (Medtronic, Minneapolis, Minn) ( $28 \pm 1$  mm), 10 with Contour 3D rigid ring (Medtronic) ( $29 \pm 1$  mm), 10 with hybrid Tri-Ad Adams band (Medtronic) ( $28 \pm 1$  mm), and 10 had no prosthesis (control group). Pressure sensors were inserted in the left ventricle, right ventricle, and right atrium. Data were acquired with open chest after weaning off cardiopulmonary bypass and hemodynamic stabilization. Annular area, global and regional contraction, height, and strain were calculated based on cubic spline fits to crystal locations.

**Results:** Tricuspid annular area contraction during the cardiac cycle was  $11\% \pm 3\%$  in the control group. The Contour 3D ring significantly impaired annular contraction ( $2\% \pm 1\%$ ) whereas the Duran AnCore ring and Tri-Ad Adams band ( $9\% \pm 3\%$  and  $8\% \pm 4\%$ , respectively) permitted dynamic area change. Global perimeter reduction was  $6\% \pm 1\%$  in the control group and decreased in the Duran AnCore ( $3\% \pm 1\%$ ), Contour 3D ( $0.4\% \pm 0.2\%$ ), and Tri-Ad Adams ( $3\% \pm 1\%$ ) groups (all  $P$  values  $< .001$  vs control). Annular height was  $6.2 \pm 2.0$  mm in the control group, unchanged in the Contour 3D ( $4.9 \pm 1.1$  mm) but reduced in the Duran AnCore ( $3.1 \pm 1.3$  mm) and Tri-Ad Adams ( $3.1 \pm 1.0$  mm) groups ( $P < .001$  Duran AnCore and Tri-Ad Adams vs control). Rings perturbed systolic global annular strain (control,  $5.3\% \pm 1.8\%$ ; Duran AnCore,  $2.3\% \pm 1.0\%$ ; Contour 3D,  $0.6\% \pm 0.2\%$ ; and Tri-Ad Adams,  $-2.6\% \pm 0.7\%$ ) with Contour 3D inducing the biggest change ( $P < .05$  vs other groups).

**Conclusions:** In healthy ovine hearts, flexible and hybrid rings better preserved annular dynamics and strain, whereas the rigid ring maintained 3-dimensional geometry. These data may aid the design of optimal tricuspid annular prostheses and improve durability of valve repair. (J Thorac Cardiovasc Surg 2021;161:e191-207)



Sonomicrometry crystals sutured to the tricuspid annulus and onto the right ventricle.

## Central Message

Tricuspid annuloplasty rings differentially impact the tricuspid annulus with rigid prostheses perturbing annular dynamics and flexible altering annular geometry. All rings affected annular strains.

## Perspective

Currently available tricuspid annuloplasty rings differ vastly in their design and material properties that may affect durability of tricuspid valve repair. Detailed analysis of the influence of prosthetic reduction on tricuspid annular dynamics, geometry, and strain may drive optimal device design to promote long-term repair durability.

See Commentaries on pages e209 and e211.

From the <sup>a</sup>Division of Cardiothoracic Surgery, Spectrum Health, Grand Rapids, Mich; <sup>b</sup>Department of Cardiac Surgery, Medical University of Silesia School of Medicine in Katowice, Katowice, Poland; <sup>c</sup>Department of Cardiac, Vascular, and Endovascular Surgery and Transplantology, Medical University of Silesia School of Medicine in Katowice, Silesian Centre for Heart Diseases, Zabrze, Poland; and <sup>d</sup>Department of Aerospace Engineering and Engineering Mechanics and Biomedical Engineering, Institute for Computational Engineering and Science, University of Texas at Austin, Austin, Tex.

Supported by a Meijer Heart and Vascular Institute internal grant.

Drs Malinowski and Jazwiec are the Peter C. and Pat Cook Endowed Research Fellows in Cardiothoracic Surgery.

Read at the 99th Annual Meeting of The American Association for Thoracic Surgery, Toronto, Ontario, Canada, May 4-7, 2019.

Received for publication May 1, 2019; revisions received Sept 6, 2019; accepted for publication Sept 9, 2019; available ahead of print Sept 28, 2019.


Address for reprints: Tomasz A. Timek, MD, PhD, Division of Cardiothoracic Surgery, Meijer Heart and Vascular Institute at Spectrum Health, 100 Michigan Ave, SE, Grand Rapids, MI 49503 (E-mail: [Tomasz.Timek@spectrumhealth.org](mailto:Tomasz.Timek@spectrumhealth.org)). 0022-5223/\$36.00

Copyright © 2019 by The American Association for Thoracic Surgery

<https://doi.org/10.1016/j.jtcvs.2019.09.060>

**Abbreviations and Acronyms**

3D	= 3 dimensional
AHCWR	= annular height to commissural ratio
ANOVA	= analysis of variance
A-P	= anteroposterior
CPB	= cardiopulmonary bypass
ECG	= echocardiogram
ED	= end-diastole
S-L	= septolateral
TR	= tricuspid regurgitation
TV	= tricuspid valve

 Video clip is available online.

More than 1.6 million Americans experience functional tricuspid regurgitation (TR),<sup>1</sup> which is a poor prognostic factor in patients with any concomitant heart disease.<sup>2</sup> Tricuspid valve (TV) annuloplasty with artificial rings currently represents the gold standard in the surgical treatment of functional TR, but despite advancements in surgical techniques and prosthesis design, a significant number of patients still present with recurrent TR after annuloplasty repair.<sup>3</sup> Several tricuspid annuloplasty prostheses are available and can be categorized based on their 3-dimensional (3D) shape (planar or nonplanar) and material properties (rigid, partially rigid, semi-rigid, or flexible). Decades of laboratory and clinical research on the mitral valve have demonstrated the importance of annuloplasty shape<sup>4,5</sup> and appropriate flexibility<sup>6</sup> in achieving good long-term results. Rigid rings are believed to provide desired annular shape remodeling but sacrifice annular contractile function, whereas flexible prostheses, at least partially, may better preserve physiologic annular dynamic parameters. Numerous studies have reported clinical outcomes of functional TR repair with various tricuspid prostheses,<sup>7,8</sup> yet little is known how the shape and material properties of an annuloplasty device influences the tricuspid annulus. Filling this knowledge gap may improve surgical results and prevent the still high recurrence rate of the tricuspid insufficiency after repair.<sup>3</sup>

Our goal was to assess the effect of flexible (Duran AnCore), rigid (Contour 3D), and hybrid (ie, flexible, semi-rigid) (Tri-Ad Adams) (Medtronic, Minneapolis, Minn)

tricuspid annuloplasty rings on annular geometry, dynamic parameters, and strains in healthy ovine hearts.

**METHODS****Surgical Preparation**

All animals received humane care in compliance with the Principles of Laboratory Animal Care formulated by the National Society for Medical Research and the Guide for Care and Use of Laboratory Animals. The study protocol was approved by our local institutional animal care and use committee (protocol No. 2017-05)

Forty healthy adult Dorset castrated male sheep (59 ± 7 kg) had external right jugular intravenous catheter placed under local anesthesia with 1% lidocaine injected subcutaneously. Animals were then anesthetized with propofol (2-5 mg/kg administered intravenously), intubated, and mechanically ventilated. General anesthesia was maintained with inhalational isoflurane (1%-2.5%). Fentanyl (5-20 µg/kg/min) was infused as additional maintenance anesthesia. A 4-Fr vascular access sheath was introduced through left carotid artery for arterial blood pressure measurements. Animals were fully heparinized and the right carotid artery and right internal jugular vein were exposed in preparation for cardiopulmonary bypass (CPB). The operative procedure was performed through a sternotomy and the heart was exposed in a pericardial cradle. Caval snares were placed and the superior and inferior vena cava cannulated with a multistage venous cannula via the right jugular vein. While on CPB and with the heart beating, both cava were snared, the right atrium opened, and 6 2-mm sonomicrometry crystals (Sonometrics Corp, London, Ontario, Canada) implanted with 5-0 polypropylene suture around the tricuspid annulus. One crystal was implanted at each commissure and an additional crystal equidistant between the commissures defining 3 annular regions (anterior, posterior, and septal) (Figure 1, A).

Duran AnCore (n = 10), Contour 3D (n = 10) and TriAd Adams (n = 10) tricuspid annuloplasty prostheses were implanted in 3 different groups of sheep around the tricuspid annulus following manufacturer's recommendations using 2-0 Ethibond sutures (J&J Medical Devices, Irvine, Calif) (Figure 1, B). Ten animals had no ring implanted and served as control. All annuloplasty rings were true-sized based on the intercommissural distance from anteroseptal to posteroseptal commissures and area of the anterior leaflet. Four additional crystals were implanted on the right ventricular epicardium along the midright ventricular free wall with a fifth crystal at the right ventricular apex. An echocardiogram (ECG) electrode connected to the sonomicrometry system was sutured to the right ventricular free wall. Pressure transducers (PA4.5-X6; Konigsberg Instruments Inc, Pasadena, Calif) were placed in the left ventricle and right ventricle through the apex with an additional pressure transducer placed in the right atrium. After completion of crystal implantation, the atriotomy was closed and the animal weaned from CPB. Animals were allowed to stabilize for 30 minutes to achieve steady state hemodynamic parameters after weaning from CPB. Every animal received 300 mg amiodarone intravenously and was maintained on lidocaine intravenous drip (0.03 mg/kg/min) to prevent ventricular ectopy. All animals were studied under open-chest experimental conditions, and simultaneous hemodynamic and sonomicrometry data were acquired.

At the conclusion of the experiment, the animals were put to death by intravenously administering sodium pentothal (100 mg/kg) and potassium chloride intravenous bolus (80 mEq). The heart was excised and the proper placement of crystals was confirmed.

**Data Acquisition**

All sonomicrometry data were acquired using a Sonometrics Digital Ultrasonic Measurement System DS3 (Sonometrics Corp) as previously described.<sup>9</sup> Data were acquired at 128 Hz with simultaneous left ventricular pressure, right ventricular pressure, central venous pressure, and ECG recordings. Data from 3 consecutive cardiac cycles during normal sinus

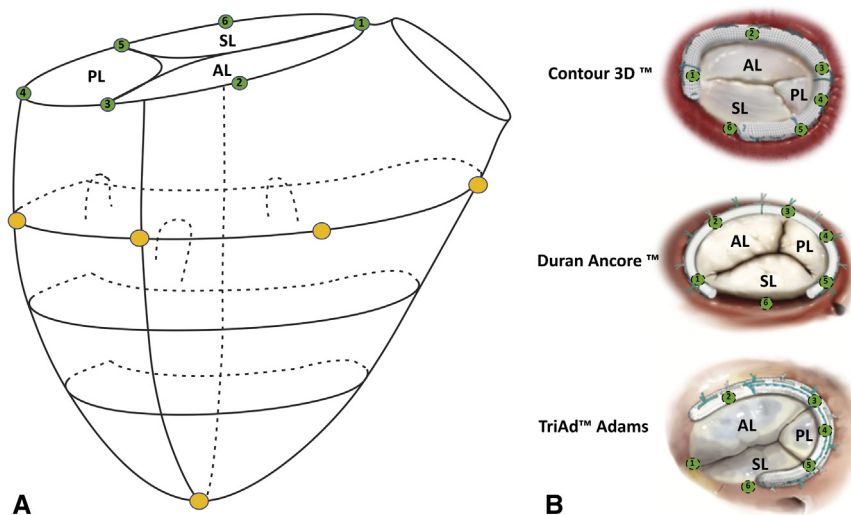


**FIGURE 1.** A, The location of the sonomicrometry crystals implanted on the tricuspid annulus (green) and right ventricle (yellow). B, The relation of annuloplasty rings to the implanted annular crystals. The sonomicrometry crystals were sutured to the native tricuspid and covered by prosthetic rings implanted. PL, Posterior leaflet; SL, septal leaflet; AL, anterior leaflet.

rhythm were averaged for each animal. All sonomicrometry recordings were analyzed with custom MATLAB code (MathWorks, Natick, Mass). All values were calculated at end-systole, end-diastole (ED), and during maximal and minimal area time. ED was defined as the time of the beginning of positive deflection in ECG voltage (R wave), whereas end-systole was determined as the time of maximum negative dp/dt of left ventricular pressure.

**Data Analysis**

**Tricuspid annular geometry and dynamics.** Tricuspid annular area and perimeter were calculated based on spline fit of annular crystals as previously described.<sup>10,11</sup> Briefly, piecewise cubic Hermitian splines that minimize the distance to the crystals and meet a minimum mathematical smoothness requirement were obtained. The spline is a

function of the arc-length parameter and time. Septolateral (S-L) annular dimension was calculated as the distance between crystals 2 and 6; anteroposterior (A-P) annular dimension as the distance between crystals 1 and 4. Intercommissural distances were calculated as the respective individual distances between crystals 1, 3, and 5 (Figure 1).

Annular 3D geometry was represented by annular height defined as the plane-normal distance between the 2 maximally displaced annular crystals above and below the best-fit annular plane. Annular height to commissural width ratio (AHCWR) was calculated as the ratio of maximal (diastolic) and minimal (systolic) displacement of annular crystals from annular plane (height) to its appropriate A-P diameter.

Annular area contraction was characterized as the percentage difference between maximal and minimal annular area during the cardiac cycle ( $[A_{max} - A_{min}] / A_{min} \times 100\%$ ). Regional annular contraction was defined

**TABLE 1. Group characteristics,\* hemodynamic parameters, and right ventricular function**

	Control (n = 10)	Duran AnCore (n = 10)	Contour 3D (n = 10)	TriAd Adams (n = 10)	P value†
Animal weight (kg)	53 ± 5	63 ± 4‡,§	66 ± 5‡,§	56 ± 4	<.001
Ring size	–	29 (27-29)	30 (28-30)§	28 (26-28.5)	.017
CPB time (min)	79 ± 6	107 ± 11‡,§	118 ± 20‡,§	87 ± 11	<.001
HR (min <sup>-1</sup> )	84 ± 13	91 ± 11	89 ± 10	81 ± 7	.199
LVP max (mm Hg)	89 (81-91)	100 (94-104)†	100 (95-110)†	95 (82-98)	.005
LVP EDP (mm Hg)	9 ± 3	10 ± 6	11 ± 3	13 ± 5	.348
RVP max (mm Hg)	24 (19-28)	22 (19-27)	21 (19-24)	24 (21-28)	.639
RV EDP (mm Hg)	7 ± 2	5 ± 2	5 ± 3	4 ± 2	.054
RV EDV <sub>ind</sub> (mL)	77 ± 13	55 ± 13†	71 ± 9	58 ± 15†	.003
RV FVC (%)	21 ± 4	26 ± 5	27 ± 5	26 ± 4	.081
RAP (mm Hg)	11 ± 5	11 ± 3	12 ± 4	7 ± 4	.059

Values are presented as mean ± standard deviation or median (interquartile range [25th-75th percentile]). CPB, Cardiopulmonary bypass; HR, heart rate; LVP, left ventricular pressure; EDP, end diastolic pressure; RVP, right ventricular pressure; RV, right ventricle; EDV<sub>ind</sub>, indexed end diastolic volume; FVC, fractional volume change; RAP, right atrial pressure. \*Duran AnCore, Contour 3D, and TriAd Adams (Medtronic, Minneapolis, Minn). †P values from analysis of variance or analysis of variance on ranks. ‡P <.05 versus control group. §P <.05 versus TriAd Adams group from post hoc pairwise multiple comparisons. All multiple comparisons results are shown in Table E1.

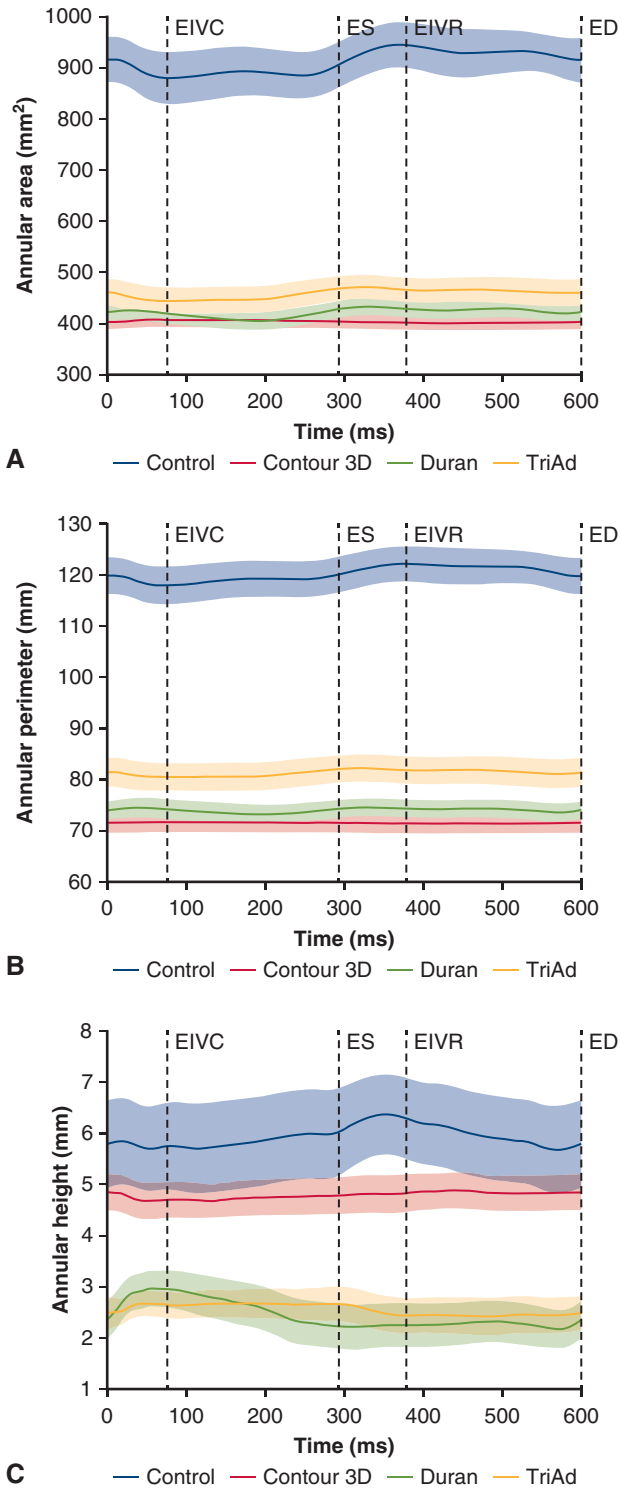


**FIGURE 2.** Tricuspid annula. A, Area. B, Perimeter. C, Height change throughout the cardiac cycle end-diastole to end-diastole (ED-ED) in all study groups. The parameters were calculated based on spline fit of annular crystals. Annular height was calculated as the distance between the 2 maximally displaced annular crystals above and below the annular plane. Data are presented as mean (solid line) ± standard error (shaded area) for the control group and after the implantation of each studied ring. EIVC, End of isovolumic contraction; ES, end-systole; EIVR, end of isovolumic relaxation.

as the percentage difference between maximal and minimal regional perimeter. Right ventricle volume was calculated using convex hull method based on crystals coordinates.

**Annular strains.** Tricuspid annular strains were calculated as previously described.<sup>11,12</sup> The strain, calculated as a relative measure of displacement and thus annular deformation, was calculated relative to a reference configuration. For the within the group global strain analysis, maximal valve area time was chosen as the reference configuration assuming it is a state of minimal annular stress. In the regional analysis, ED was chosen as the reference configuration to uniform the representation of strain change during the cardiac cycle. Between group analysis included averaged control group ED, end of isovolumic contraction, end-systole, end of isovolumic relaxation, and maximal and minimal valve area times as the reference for respective time points in the ring groups. Therefore, cardiac strain (within group) reflects the deformation of the annulus throughout the cardiac cycle in each group and ring strain (between groups) reflects the deformation of the annulus induced by ring implantation. Specifically, Green-Lagrange strain was calculated along the entire annulus for each animal and later displayed on a spline representation of the population averaged annulus for each group. Global and regional average tricuspid annular strains were calculated for the entire annulus and the anterior, posterior, and septal annulus by averaging them along the respective regions. Negative or compressive strains imply that tissue is compressed, whereas positive or tensile strains imply that tissue is stretched

**Statistical Analysis**

**Sample size calculation.** Data were planned to be analyzed using analysis of variance (ANOVA) with a type I error level of 5%. Similar previous studies on the mitral valve revealed that the implantation of annuloplasty rings results in the decrease in annular contractility from 17% ± 6% to 3% ± 1% and from 20% ± 7% to 6% ± 3% with rigid and flexible rings, respectively.<sup>13,14</sup> Proving previously that tricuspid annulus is similarly active structure, we showed its normal contractility of 12% ± 5%.<sup>12</sup> We expected to observe at least 60% annular contractility reduction with a mean difference of 8.5% with supposedly similar as observed earlier standard deviation of 5%. To detect such a difference with the 80% power we needed 9 animals. The final sample size was determined adjusting the size for possible animal attrition (1 animal per group). That led us to the final sample size of 10 sheep per group.

Values are presented as mean ± 1 when normally distributed or as median with 25th and 75th percentiles when normality assumptions (Shapiro-Wilk test) were not met. Because of the difference in animal weight between the groups (Table 1) all geometric distances presented were indexed to individual animal body weight and normalized to the mean weight of studied population. The measured variables were compared between the groups using 1- way ANOVA or nonparametric Kruskal-Wallis ANOVA on ranks. If P value from ANOVA was significant (P < .05) then pairwise multiple comparisons were performed with Holm-Sidak or Dunn post hoc test, respectively. Each P value from post hoc analysis was adjusted appropriately to account for multiple comparisons with the familywise significance and confidence level α = 0.05. The strain results were analyzed similarly. SigmaPlot 12.5 (SYSTAT, San Jose, Calif) was used for normality testing and sample size calculation; GraphPad Prism 8.2.0 (GraphPad Software, San Diego, Calif) was used for the ANOVA.

**RESULTS**

**Hemodynamic Characteristics**

Operative and hemodynamic characteristics for each animal group are presented in Tables 1 and E1. There was no difference in heart rate and right ventricular function between the groups, but right ventricular indexed volume

TABLE 2. Tricuspid annular diameters by group\*

	Control (n = 10)	Duran AnCore (n = 10)	Contour 3D (n = 10)	TriAd Adams (n = 10)	P value†
S-L diameter (mm)					
Maximal	33.6 (32.0-35.4)	19.8 (18.5-23.4)‡	19.0 (18.2-21.2)‡	20.6 (18.8-21.7)‡	<.001
Minimal	31.0 ± 2.0	19.7 ± 3.0‡	19.4 ± 2.4‡	20.1 ± 3.2‡	<.001
Shortening (%)	5.3 (4.4-13.7)§	5.9 (4.8-6.9)§	1.0 (0.5-1.3)‡	3.9 (3.2-5.4)§	<.001
A-P diameter (mm)					
Maximal	36.7 ± 2.6	22.7 ± 2.3‡	24.6 ± 1.7‡	27.8 ± 3.3‡,§	<.001
Minimal	33.8 ± 3.7	22.3 ± 2.4‡	24.5 ± 1.7‡	26.6 ± 3.5‡	<.001
Shortening (%)	10.1 (3.0-12.9)	2.6 (2.0-3.4)	0.4 (0.2-0.8)‡	4.4 (2.0-6.1)§	<.001
C-C 1-3 (mm)					
Maximal	29.5 ± 2.8	16.4 ± 2.2‡,§	21.5 ± 1.6‡	21.3 ± 2.3‡	<.001
Minimal	26.7 ± 2.3	16.2 ± 2.2‡,§	21.3 ± 1.6‡	19.7 ± 2.2‡	<.001
Shortening (%)	8.8 (5.9-13.9)	1.5 (0.7-2.3)‡	0.6 (0.4-0.8)‡	6.3 (4.3-11.9)§	<.001
C-C 3-5 (mm)					
Maximal	32.4 (22.3-41.8)	17.9 (16.3-19.9)‡	13.6 (12.3-18.8)‡	20.4 (16.6-22.7)	<.001
Minimal	30.8 (21.5-40.7)	17.7 (16.2-19.7)‡	13.5 (12.2-16.7)‡	20.1 (16.2-22.5)	<.001
Shortening (%)	3.7 ± 1.1	1.7 ± 1.0‡,§	0.6 ± 0.4‡	1.2 ± 0.7‡	<.001
C-C 5-1 (mm)					
Maximal	40.8 ± 5.4	26.8 ± 2.4‡,§	23.1 ± 2.3‡	27.9 ± 2.6‡,§	<.001
Minimal	37.5 ± 5.3	25.9 ± 2.5‡	22.9 ± 2.3‡	26.9 ± 2.7‡,§	<.001
Shortening (%)	7.3 (5.3-11.9)	2.9 (2.3-3.5)§	0.6 (0.4-1.1)‡	3.0 (2.0-4.9)§	<.001

Values are presented as mean ± standard deviation or median (interquartile range [25th-75th percentile]). Crystal numbers as depicted in Figure 1: Crystal #1, antero-septal commissure; crystal #3, anteroposterior commissure; crystal # 5, posteroseptal commissure. S-L, Septo-lateral; A-P, antero-posterior; C-C, intercommissural distances. \*Duran AnCore, Contour 3D, and TriAd Adams (Medtronic, Minneapolis, Minn). †P values from analysis of variance or analysis of variance on ranks. ‡P < .05 versus control group. §P < .05 versus contour 3D group from post hoc pairwise multiple comparison. All multiple comparisons results are shown in Table E3.

was significantly smaller in Duran AnCore and TriAd Adams groups than in the control group. Maximal left ventricular pressure was higher in Duran AnCore and Contour 3D group animals than in control group animals.

### Tricuspid Annular Geometry and Dynamic Parameters

The maximal tricuspid annular area in the diastole was  $967 \pm 142 \text{ mm}^2$  in the control group and decreased to  $441 \pm 61 \text{ mm}^2$ ,  $408 \pm 46 \text{ mm}^2$ , and  $476 \pm 83 \text{ mm}^2$  in Duran AnCore, Contour 3D, and TriAd Adams groups, respectively ( $P < .001$  all groups vs control group). Minimal annular area during systole was  $880 \pm 146 \text{ mm}^2$  in the control group and  $403 \pm 55 \text{ mm}^2$ ,  $401 \pm 46 \text{ mm}^2$ , and  $434 \pm 89 \text{ mm}^2$  in Duran AnCore, Contour 3D, and TriAd Adams rings, respectively (all  $P$  values < .001 vs control group). Tricuspid annular area change during the cardiac cycle was median 10% (IQR, 9%-12%) in the control group, was maintained with Duran AnCore (median, 8%; IQR, 7%-11%) and TriAd Adams (median, 7%; IQR, 6%-12%), but was severely impaired with the Contour 3D ring (median, 2%; IQR, 1%-2%) ( $P < .001$  Contour 3D vs control, Duran AnCore, and TriAd Adams) (Table E2). The change of annular area and perimeter throughout the cardiac cycle in each animal group is shown in

Figure 2. The maximal and minimal S-L, A-P, and intercommissural annular distances are illustrated in Table 2 and all detailed comparisons are shown in Table E3. The rigid Contour 3D ring abolished both S-L and A-P annular reduction during cardiac cycle, whereas the flexible Duran AnCore band and the TriAd Adams prosthesis maintained S-L and A-P annular shortening.

Implantation of any annular prosthesis perturbed regional annular dynamics: The rigid ring completely abolished contraction in all annular regions (ie, anterior, posterior, and septal). Both in flexible Duran AnCore and hybrid TriAd Adams rings, the annular segments not covered by the prosthetic material (septal crystals 5 and 6 in Duran AnCore, anterior crystals 1 and 2 in TriAd Adams, and septal segment 6-1 in both) maintained their physiologic contractility comparable to control group contractility (Figure 3 and Table E4).

Normal 3D geometry of the native tricuspid annulus was perturbed by device implantation. The saddle-like shape with high points near antero-septal commissure and mid-posterior annulus observed in the control group was altered by flexible and hybrid semirigid rings. Maximal annular height was  $6.2 \pm 2.0 \text{ mm}$  in the control group and remained unaltered with the Contour 3D ring ( $4.9 \pm 1.1 \text{ mm}$ ) but decreased with both Duran AnCore ( $3.1 \pm 1.3 \text{ mm}$ ) and

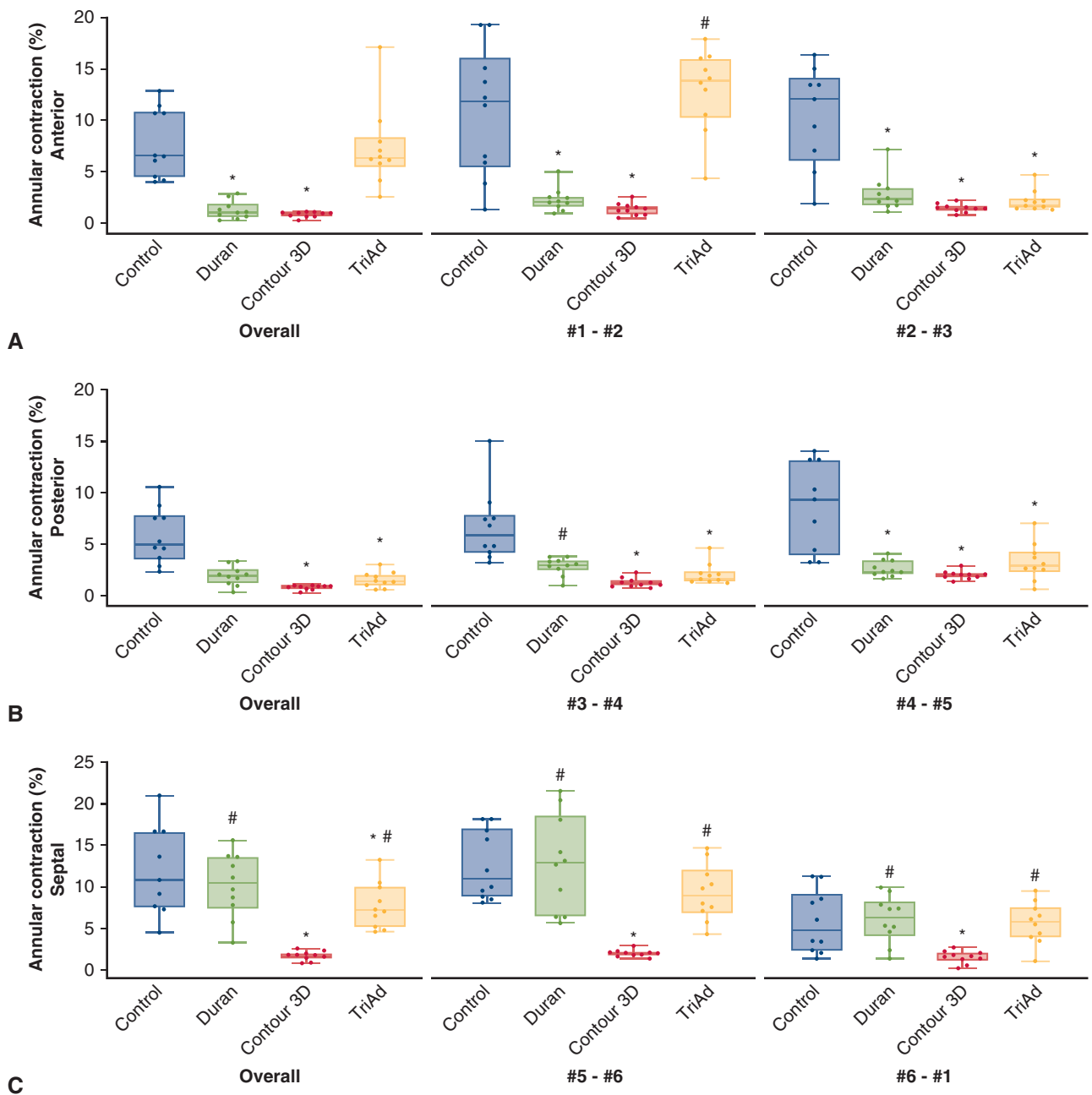


**FIGURE 3.** Regional tricuspid annular contraction in the control and after the implantation of each studied ring. Contraction was calculated as the percent difference between maximal and minimal regional perimeter. Crystal numbers (#1-6) as depicted in Figure 1. A, Anterior annulus (crystals #1, #2, #3). B, Posterior annulus (crystals #3, #4, #5). C, Septal annulus (crystals #5, #6, #1). The upper and lower borders of the box represent the upper and lower quartile. The middle horizontal line represents the median. The upper and lower whiskers represent the maximum and minimum values. P values from analysis of variance. \*P < .05 versus control group. #P < .05 versus Contour3D (Medtronic, Minneapolis, Minn) group. See Table E4 for detailed results of multiple comparisons.

TriAd Adams prostheses ( $3.1 \pm 1.0$  mm) ( $P < .001$  Duran AnCore and TriAd Adams vs control). Annular height changed dynamically during the heart cycle (Figure 2) in control ( $23\% \pm 16\%$ ), Duran AnCore ( $21\% \pm 13\%$ ), and TriAd Adams ( $22\% \pm 14\%$ ) but significantly less so with the Contour 3D ring ( $7\% \pm 3\%$ ;  $P = .037$  vs control).

AHCWR during diastole at maximal valve area time was  $17\% \pm 6\%$  in control and  $19\% \pm 4\%$  in Contour 3D ( $P = .759$  vs control) but was reduced to  $11\% \pm 6\%$  and  $10\% \pm 4\%$  for Duran AnCore and TriAd Adams, respectively ( $P < .03$  vs control and Contour 3D). During systole AHCWR at minimal valve area time in the control group

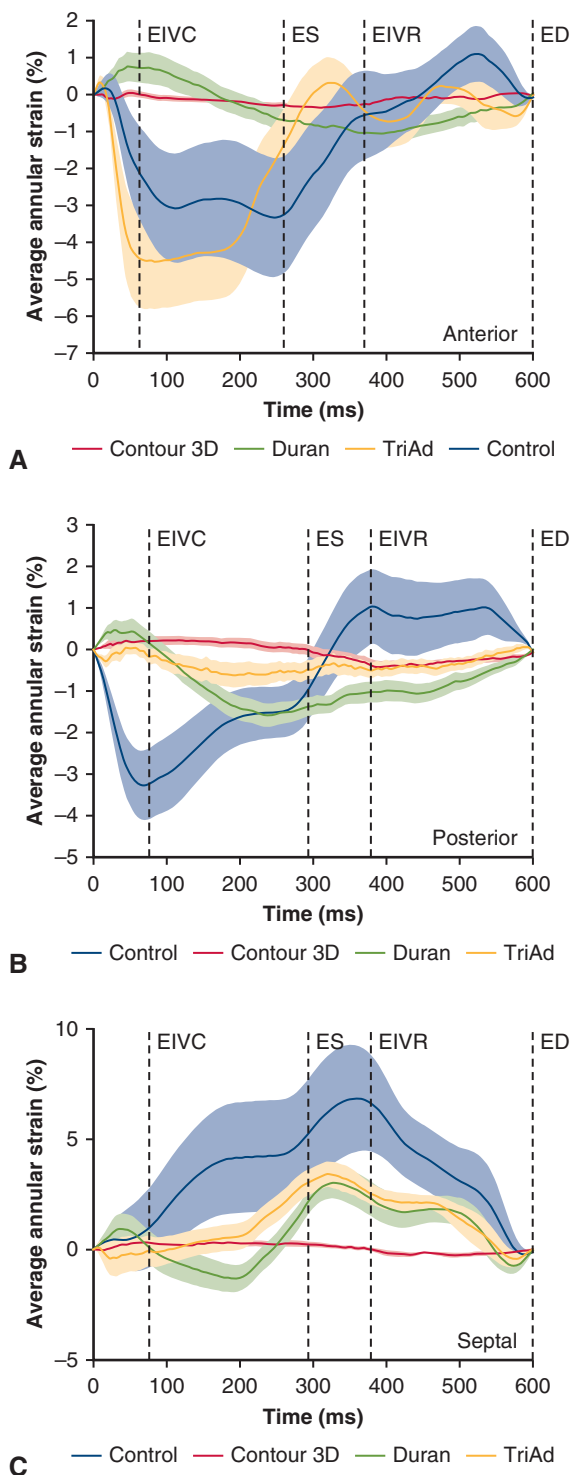


**FIGURE 4.** Regional average annular cardiac strains in the control and with the implanted rings shown throughout the entire cardiac cycle (end-diastole to end diastole [ED-ED]). A, Anterior. B, Posterior. C, Septal tricuspid annulus. Strain pattern showed severely attenuated magnitude of strain by the rigid ring in all regions. Data are presented as mean (solid lines)  $\pm$  standard error (shaded areas). EIVC, End of isovolumic contraction; ES, end-systole; EIVR, end of isovolumic relaxation.

was  $16\% \pm 7\%$  and  $20\% \pm 4\%$  in the Contour 3D group ( $P = .160$  vs control). It was smaller with Duran AnCore ( $11\% \pm 5\%$ ) and TriAd Adams ( $10\% \pm 3\%$ ) when comparing to the rigid ring ( $P < .002$  vs Contour 3D) (Table E2).

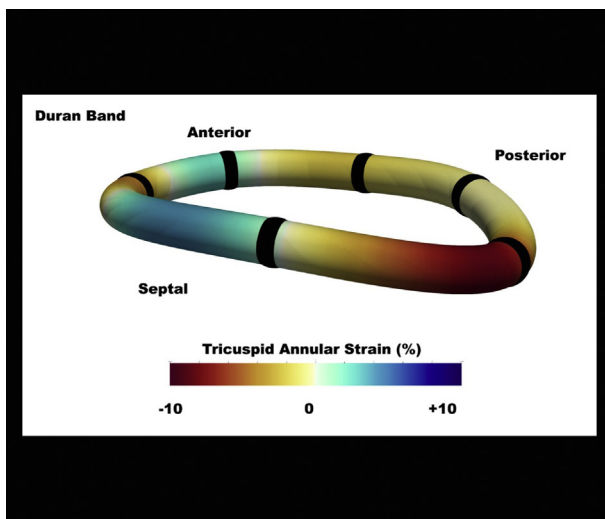
**Tricuspid Annular Strains**

The global averaged systolic annular strain was  $-5.3\% \pm 1.8\%$  in the control group and was most perturbed by the Contour 3D ring ( $-0.6\% \pm 0.2\%$ ;  $P < .001$  vs control). Duran AnCore ( $-2.3\% \pm 1.0\%$ ) and TriAd Adams ( $-2.6\% \pm 0.7\%$ ) prostheses diminished the magnitude of global strain to similar degree ( $P < .005$  vs control and Contour 3D) (Table E2). Detailed analysis of regional cardiac strain pattern confirmed severely attenuated magnitude of strain by the rigid nonplanar Contour 3D ring in all regions. The TriAd Adams ring did not alter anterior annular strain but significantly diminished posterior annular strain. The Duran AnCore band decreased magnitude of both anterior and posterior annular strain (Figure 4).

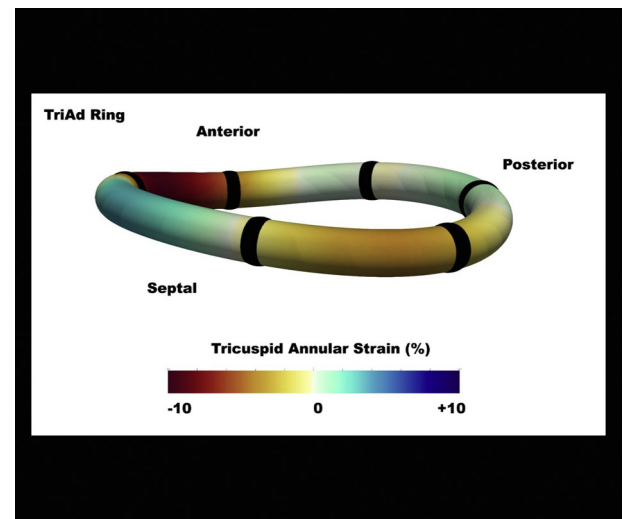
An interesting finding was the systolic annular stretch observed in the septal region of control animals. This pattern was slightly decreased by the TriAd Adams ring, abolished by the Contour 3D device, and reversed to systolic contraction by the Duran AnCore prosthesis (Figure 4, C). Cardiac annular strain with implanted rings in 3 consecutive heart cycles is shown in Video 1 (Duran AnCore), Video 2 (Contour 3D), and Video 3 (TriAd Adams). The implantation of any ring caused significant annular compression in relation to the normal native annulus (Figure 5). Least compression was observed in the region not covered by the ring in the Duran AnCore group, whereas the largest compression was present in the unsupported region of the rigid ring. The TriAd Adams ring induced significant annular compression along the anterior and posterior annulus.

**DISCUSSION**

The results of our study revealed differential effects of 3 distinct annuloplasty devices (Duran AnCore, Contour 3D, and TriAd Adams) on tricuspid annular geometry and dynamic parameters. The rigid, nonplanar Contour 3D ring diminished global and regional physiologic annular contraction but best preserved normal annular geometry. The flexible Duran AnCore and the hybrid semirigid TriAd Adams rings spared annular area contraction and dynamic parameters of the septal annulus but decreased annular nonplanarity. All rings perturbed global annular strains and similarly decreased all annular dimensions. The tricuspid annulus, similar to the mitral annulus, is a 3D, saddle-like structure with its high points near anteroseptal commissure and midposterior annulus.<sup>10</sup> Its nonplanar shape has been confirmed in both experimental animals and humans

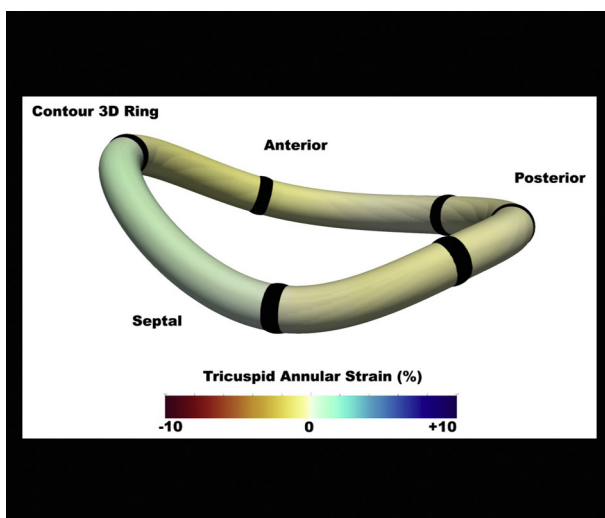


**VIDEO 1.** Tricuspid annular strain after the implantation of Duran AnCore band (Medtronic, Minneapolis, Minn). Video available at: [https://www.jtcvs.org/article/S0022-5223\(19\)32061-6/fulltext](https://www.jtcvs.org/article/S0022-5223(19)32061-6/fulltext).



**VIDEO 3.** Tricuspid annular strain after the implantation of TriAd Adams ring (Medtronic, Minneapolis, Minn). Video available at: [https://www.jtcvs.org/article/S0022-5223\(19\)32061-6/fulltext](https://www.jtcvs.org/article/S0022-5223(19)32061-6/fulltext).

utilizing detailed sonomicrometry measurements and various clinical imaging modalities, including 3D ECG and magnetic resonance imaging.<sup>9,10,15,16</sup> The complex 3D geometry of the tricuspid annulus may play a role in reducing leaflet stress, as has been postulated for the saddle-like shape of the mitral annulus.<sup>4</sup> This putative influence of annular geometry may be more important on the right side because we recently reported ovine tricuspid leaflet strains in vivo that were much higher than those observed in the mitral valve.<sup>17</sup> As such, alterations of annular geometry through prosthetic reduction may have a more pronounced effect on valvular stresses. Functional



**VIDEO 2.** Tricuspid annular strain after the implantation of Contour 3D ring (Medtronic, Minneapolis, Minn). Video available at: [https://www.jtcvs.org/article/S0022-5223\(19\)32061-6/fulltext](https://www.jtcvs.org/article/S0022-5223(19)32061-6/fulltext).

TR similar to the mitral valve has been found to be associated with flattening of the annulus and clinical studies suggest that restoration of bimodal annular shape and not annular reduction alone is critical to effective TR repair.<sup>18</sup> This was first demonstrated in the mitral valve where the shape reconstruction was found to be beneficial.<sup>4,19</sup> Thus, the implantation of nonplanar rings to maintain annular height (as seen with the Contour 3D ring in our study) seems to be a reasonable approach to restore normal annular shape, especially because preservation of annular height was also shown to provide better leaflet coaptation.<sup>19</sup> Moreover, planar prostheses (both flexible and rigid) were found to aggravate TV leaflet tenting,<sup>20</sup> a known predictive parameter of residual TR after surgery.<sup>21</sup> The reduction of leaflet tethering is beneficial and improves the durability of TV repair.<sup>22,23</sup> In our study, only the Contour 3D ring preserved normal annular height, perhaps promoting better coaptation, yet in vitro studies demonstrate no difference in leaflet stretch regardless of annular shape (flat vs saddle) thus questioning this hypothesis.<sup>24</sup> To better understand the effect of ring implantation on annular geometry we analyzed the AHCWR, which we found to be unchanged with the Contour 3D ring and decreased with both Duran AnCore and TriAd Adams rings in diastole but with no change for the latter rings in systole. Preservation of normal AHCWR is believed to optimize leaflet stress<sup>4</sup> with ideal values between 15% and 30% and exponential stress increase with ratio reduction as demonstrated for the mitral valve.<sup>5</sup> If one were to extrapolate these mitral data to the tricuspid valve, use of the Contour 3D ring with its 19% to 20% AHCWR would again be favored. AHCWR in the Duran AnCore group in diastole was reduced due to both A-P diameter decrease and the annular flattening,



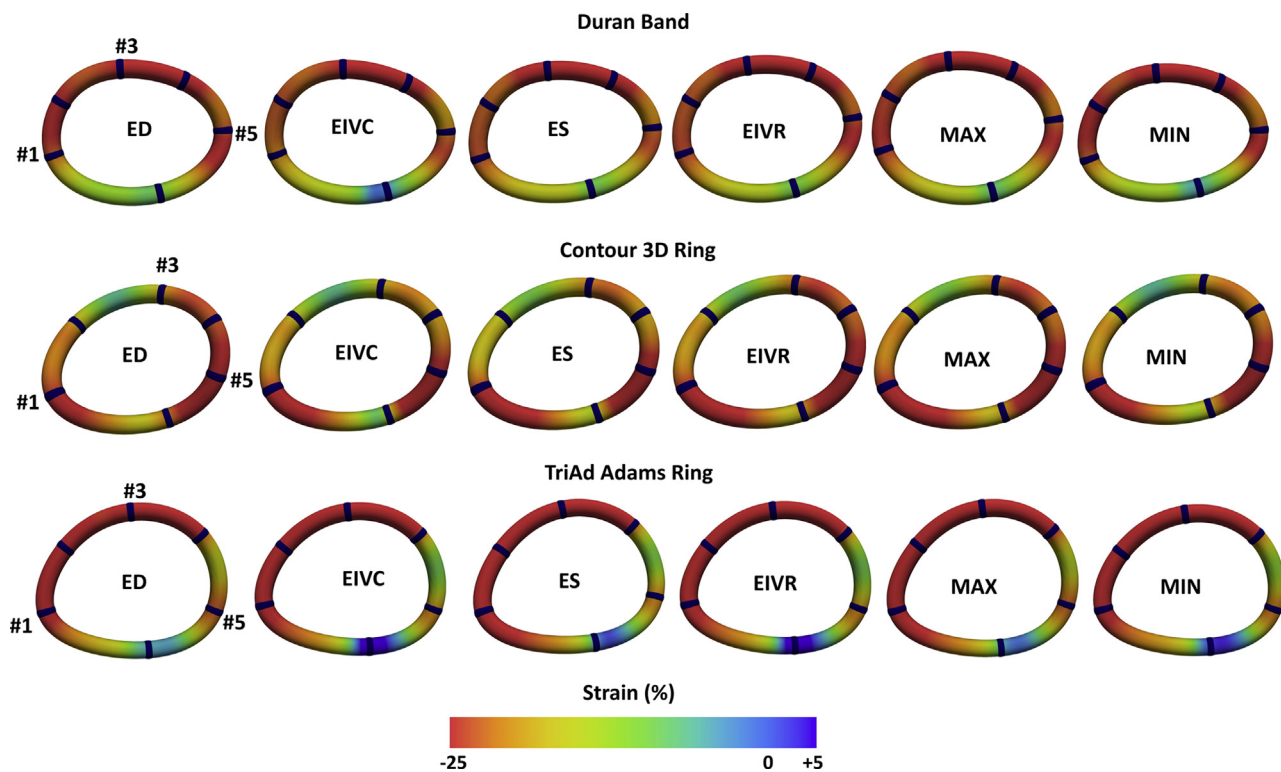


**FIGURE 5.** Average tricuspid annular strains with the implanted rings. The metric is shown on the average annular spline. The strain maps are presented in the reference to the control group at the same time point. The positive strain values indicate annular stretch, and the negative annular compression Crystals 1, 3, and 5 represent anteroseptal, anteroposterior, and posteroseptal commissures, respectively. *ED*, End-diastole; *EIVC*, end of isovolumic contraction; *ES*, end-systole; *EIVR*, end of isovolumic relaxation; *MAX*, maximal valve area time; *MIN*, minimal valve area time.

which is in contrast to the mitral valve where the Duran AnCore prosthesis was found to better preserve annular saddle shape.<sup>25</sup> This discrepancy may be attributable to the different compliance of the left and right ventricles and the use of a partial versus complete prosthesis for tricuspid and mitral annuloplasty, respectively.

The tricuspid annulus is a dynamic structure with area change during the cardiac cycle ranging from 10% to 39%<sup>10,15,26,27</sup> in animal and clinical studies. In our study, tricuspid annular area change during the cardiac cycle for normal sheep was 10% (IQR, 9%-12%). This dynamic behavior was essentially abolished with Contour 3D implantation corroborating the clinical findings of Nishi and colleagues<sup>27</sup> utilizing 3D ECG. The Duran AnCore ring better preserved annular dynamic parameters, yet Dagum and colleagues<sup>28</sup> found that flexible annular prostheses virtually eliminated mitral annular area change during the cardiac cycle regardless of whether a partial or full prosthesis was implanted. These differences may be due to the dynamic motion of the septal region of the tricuspid annulus versus the static fibrous anterior mitral annulus. The TriAd Adams ring was recently introduced with the idea of combining the concept of “annular remodeling with rigid rings, while preserving the annular motion of the flexible

bands.”<sup>29</sup> In fact, we found that this hybrid semi-rigid device preserved annular area contraction similar to the flexible band. The differential effect on anterior annular dynamics of Duran AnCore and TriAd Adams rings may be due to variance of material properties and different implantation techniques (Figure 1, B).

The influence of prosthetic annular reduction on the geometry and function of the right ventricle must also be considered. In the acute setting, all studied rings were previously shown to reduce right ventricle free wall stress,<sup>30</sup> but in the long term one may expect rigid rings to result in more complete right ventricular reverse remodeling, as reported by Gatti and colleagues.<sup>31</sup> However, rigid nonplanar rings have been associated with higher risk of prosthesis dehiscence.<sup>8</sup> Influence of the Contour 3D ring on annular strains seen in our study corroborates these clinical observations.

Cardiac cycle strains for the native ovine annulus presented in this study are in agreement with previous reports.<sup>11</sup> To our best knowledge, our study is the first to describe the effect of annuloplasty rings on tricuspid annular strains. Based on prior experimental reports of mitral annular strains after ring annuloplasty,<sup>32</sup> significant alterations of tricuspid annular strain after prosthetic

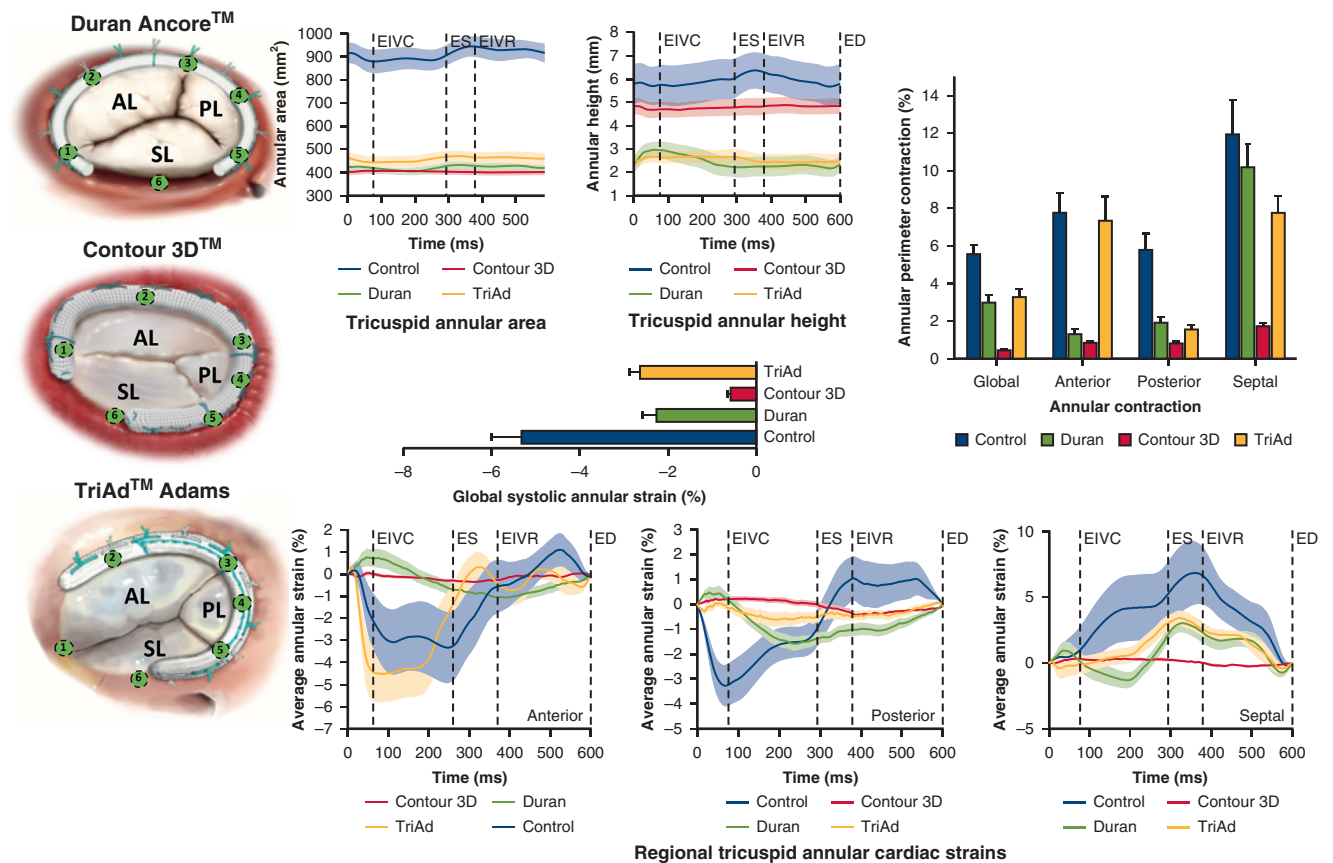


**FIGURE 6.** Tricuspid annular geometry, dynamics, and strain changes after the implantation of flexible (Duran AnCore), rigid (Contour 3D) and hybrid (TriAd Adams) tricuspid annuloplasty rings (Medtronic, Minneapolis, Minn). The parameters were calculated based on the 3-dimensional coordinates of 6 implanted onto the native annulus sonomicrometry crystals. All studied annuloplasty devices perturbed tricuspid annular geometry, dynamics, and global and regional strain. The Contour 3D rigid nonplanar ring maintained 3-dimensional geometry of the native annulus while abolishing annular dynamic parameters and decreasing the magnitude of cardiac strains. The Duran AnCore and TriAd Adams rings allowed for physiologic annular area contraction but resulted in annular flattening and perturbed regional annular strain. AL, Anterior leaflet; PL, posterior leaflet; SL, septal leaflet; EIVC, end of isovolumic contraction; ES, end-systole; EIVR, end of isovolumic relaxation; ED, end-diastole.

reduction were expected. As with the mitral valve, the largest shifts were observed with rigid rings.<sup>14,32</sup> The stiff posterior portion of the TriAd Adams prosthesis displayed similar influence. Although the TriAd Adams and Duran AnCore rings were designed to preserve annular dynamic parameters, global and regional strain perturbations suggest that these dynamics are not fully physiological. Reversal of midsystolic septal annular elongation seen after Duran AnCore band implantation was an interesting finding. This physiologic phenomenon, also seen in the anterior mitral annulus<sup>14</sup> may be explained by aortic root expansion during systole. The abnormal septal and anterior tricuspid annular strain induced by the flexible band may play a role in the inferior performance and higher rates of TR recurrence after flexible band annuloplasty.<sup>33</sup> These changes are probably related to the incomplete annular fixation by the flexible material but still strong enough to influence the compliant right ventricular myocardium. But further detailed analysis of annular-

ventricular coupling is necessary to precisely describe the origin of this phenomenon.

**Study Limitations**

The results of the current study must be interpreted in light of several limitations. This was an acute animal study, and clinical extrapolation of the results must be done with extreme caution. Our experiment was performed in open-chest healthy sheep under anesthesia, but we have previously shown that the anesthesia may affect tricuspid annular dynamics but does not alter annular geometry.<sup>34</sup> The surgeries were performed on animals with normal hearts and annular size, whereas clinical annuloplasty is usually performed in hearts with right ventricle dysfunction and with a dilated tricuspid annulus. However, use of healthy animals permitted assessment of the direct effect of rings on annular dynamics and strain without potentially confounding factors related to valvular insufficiency or myocardial disease. The ultimate goal of durable valve repair is the restoration of leaflet

coaptation, but our study did not analyze the effect of prosthetic annular reduction on the subvalvular apparatus.

Because of multiple comparisons performed during statistical data analysis there is a risk of type I error that the authors acknowledge.

## CONCLUSIONS

In healthy adult sheep, all studied annuloplasty devices perturbed tricuspid annular geometry, dynamics, and strain. The Contour 3D rigid nonplanar ring maintained 3D geometry of the native annulus while abolishing annular dynamics and decreasing the magnitude of cardiac strains. The Duran AnCore and TriAd Adams rings allowed for physiologic annular area contraction but resulted in annular flattening and perturbed regional annular strain (all changes observed are presented in Figure 6). These data may guide more rational design of future annular prostheses to improve durability of surgical annuloplasty.

## Webcast

You can watch a Webcast of this AATS meeting presentation by going to: [https://aats.blob.core.windows.net/media/19%20AM/Sunday\\_May5/206BD/206BD/May5-206AB-0905-0915-Malinowski.mp4](https://aats.blob.core.windows.net/media/19%20AM/Sunday_May5/206BD/206BD/May5-206AB-0905-0915-Malinowski.mp4).

The Impact of Tricuspid Annuloplasty Prostheses on Ovine Annular Geometry and Kinematics

M. Malinowski, T. Jazwiec, M.K. Rausch\*, N. Dague, M. Goehler, T.A. Timek  
Spectrum Health, Grand Rapids, MI, USA; \*University of Texas, Austin, TX, USA



## Conflict of Interest Statement

This work was partially supported by a research grant from Medtronic Inc. Dr Rausch has a speaking agreement with Edwards Lifesciences. All other authors have nothing to disclose with regard to commercial support.

## References

- Stuge O, Liddicoat J. Emerging opportunities for cardiac surgeons within structural heart disease. *J Thorac Cardiovasc Surg.* 2006;132:1258-61.
- Agricola E, Stella S, Gullace M, Ingallina G, D'amato R, Slavich M, et al. Impact of functional tricuspid regurgitation on heart failure and death in patients with functional mitral regurgitation and left ventricular dysfunction. *Eur J Heart Fail.* 2012;14:902-8.
- McCarthy PM, Bhudia SK, Rajeswaran J, Hoercher KJ, Lytle BW, Cosgrove DM, et al. Tricuspid valve repair: durability and risk factors for failure. *J Thorac Cardiovasc Surg.* 2004;127:674-85.
- Salgo IS, Gorman JH, Gorman RC, Jackson BM, Bowen FW, Plappert T, et al. Effect of annular shape on leaflet curvature in reducing mitral leaflet stress. *Circulation.* 2002;106:711-7.
- Ryan LP, Jackson BM, Hamamoto H, Eperjesi TJ, Plappert TJ, St John-Sutton M, et al. The influence of annuloplasty ring geometry on mitral leaflet curvature. *Ann Thorac Surg.* 2008;86:749-60.
- Hu X, Zhao Q. Systematic evaluation of the flexible and rigid annuloplasty ring after mitral valve repair for mitral regurgitation. *Eur J Cardiothorac Surg.* 2011;40:480-7.
- Maghami S, Ghoreishi M, Foster N, Dawood MY, Hobbs GR, Stafford P, et al. Undersized rigid nonplanar annuloplasty: the key to effective and durable repair of functional tricuspid regurgitation. *Ann Thorac Surg.* 2016;102:735-42.
- Pfannmüller B, Doenst T, Eberhardt K, Seeburger J, Borger MA, Mohr FW. Increased risk of dehiscence after tricuspid valve repair with rigid annuloplasty rings. *J Thorac Cardiovasc Surg.* 2012;143:1050-5.
- Malinowski M, Wilton P, Khaghani A, Langholz D, Hooker V, Eberhart L, et al. The effect of pulmonary hypertension on ovine tricuspid annular dynamics. *Eur J Cardiothorac Surg.* 2016;49:40-5.
- Malinowski M, Jazwiec T, Goehler M, Quay N, Bush J, Jovinge S, et al. Sonomicrometry-derived 3-dimensional geometry of the human tricuspid annulus. *J Thorac Cardiovasc Surg.* 2019;157:1452-61.
- Rausch MK, Malinowski M, Wilton P, Khaghani A, Timek TA. Engineering analysis of tricuspid annular dynamics in the beating ovine heart. *Ann Biomed Eng.* 2018;46:443-51.
- Malinowski M, Schubert H, Wodarek J, Ferguson H, Eberhart L, Langholz D, et al. Tricuspid annular geometry and strain after suture annuloplasty in acute ovine right heart failure. *Ann Thorac Surg.* 2018;106:1804-11.
- Timek T, Dague P, Lai DT, Tibayan F, Liang D, Daughters GT, et al. Will a partial posterior annuloplasty ring prevent acute ischemic mitral regurgitation? *Circulation.* 2002;106(12 Suppl 1):I33-9.
- Rausch MK, Bothe W, Kvitting JPE, Swanson JC, Miller DC, Kuhl E. Mitral valve annuloplasty: a quantitative clinical and mechanical comparison of different annuloplasty devices. *Ann Biomed Eng.* 2012;40:750-61.
- Maffessanti F, Gripari P, Pontone G, Andreini D, Bertella E, Mushtaq S, et al. Three-dimensional dynamic assessment of tricuspid and mitral annuli using cardiovascular magnetic resonance. *Eur Heart J Cardiovasc Imaging.* 2013;14:986-95.
- Addetia K, Muraru D, Veronesi F, Jenei C, Cavalli G, Besser SA, et al. 3-Dimensional echocardiographic analysis of the tricuspid annulus provides new insights into tricuspid valve geometry and dynamics. *JACC Cardiovasc Imaging.* 2019;12:401-12.
- Mathur M, Jazwiec T, Meador WD, Malinowski M, Goehler M, Ferguson H, et al. Tricuspid valve leaflet strains in the beating ovine heart. *Biomech Model Mechanobiol.* 2019;18:1351-61.
- Ton-Nu TT, Levine RA, Handschumacher MD, Dorer DJ, Yosefy C, Fan D, et al. Geometric determinants of functional tricuspid regurgitation: insights from 3-dimensional echocardiography. *Circulation.* 2006;114:143-9.
- Jensen MO, Jensen H, Levine RA, Yoganathan AP, Andersen NT, Nygaard H, et al. Saddle-shaped mitral valve annuloplasty rings improve leaflet coaptation geometry. *J Thorac Cardiovasc Surg.* 2011;142:697-703.
- Min SY, Song JM, Kim JH, Jang MK, Kim YJ, Song H, et al. Geometric changes after tricuspid annuloplasty and predictors of residual tricuspid regurgitation: a real-time three-dimensional echocardiography study. *Eur Heart J.* 2010;31:2871-80.
- Yiu KH, Wong A, Pu L, Chiang MF, Sit KY, Chan D, et al. Prognostic value of preoperative right ventricular geometry and tricuspid valve tethering area in patients undergoing tricuspid annuloplasty. *Circulation.* 2014;129:87-92.
- Dreyfus GD, Raja SG, John Chan KM. Tricuspid leaflet augmentation to address severe tethering in functional tricuspid regurgitation. *Eur J Cardiothorac Surg.* 2008;34:908-10.
- Fukuda S, Song JM, Gillinov AM, McCarthy PM, Daimon M, Kongsarepong V, et al. Tricuspid valve tethering predicts residual tricuspid regurgitation after tricuspid annuloplasty. *Circulation.* 2005;111:975-9.
- Spinner EM, Buice D, Yap CH, Yoganathan AP. The effects of a three-dimensional, saddle-shaped annulus on anterior and posterior leaflet stretch and regurgitation of the tricuspid valve. *Ann Biomed Eng.* 2012;40:996-1005.
- Timek TA, Glasson JR, Lai DT, Liang D, Daughters GT, Ingels NB, et al. Annular height-to-commissural width ratio of annuloplasty rings in vivo. *Circulation.* 2005;112(9 Suppl):I423-8.
- Tsakiris AG, Mair DD, Seki S, Titus JL, Wood EH. Motion of the tricuspid valve annulus in anesthetized intact dogs. *Circ Res.* 1975;36:43-8.
- Nishi H, Toda K, Miyagawa S, Yoshikawa Y, Fukushima S, Kawamura M, et al. Tricuspid annular dynamics before and after tricuspid annuloplasty—three-dimensional transesophageal echocardiography. *Circ J.* 2015;79:873-9.
- Dague P, Timek T, Green GR, Daughters GT, Liang D, Ingels NB, et al. Three-dimensional geometric comparison of partial and complete flexible mitral annuloplasty rings. *J Thorac Cardiovasc Surg.* 2001;122:665-73.
- Milla F, Castillo JG, Varghese R, Chikwe J, Anyanwu AC, Adams DH. Rationale and initial experience with the Tri-Ad Adams tricuspid annuloplasty ring. *J Thorac Cardiovasc Surg.* 2012;143(4 Suppl):S71-3.

30. Jazwiec T, Malinowski M, Bush J, Goehler M, Quay N, Parker J, et al. Right ventricular free wall stress after tricuspid valve annuloplasty in acute ovine right heart failure. *J Thorac Cardiovasc Surg.* 2019;158:759-68.
31. Gatti G, Dell'Angela L, Morosin M, Maschietto L, Pinamonti B, Benussi B, et al. Flexible band versus rigid ring annuloplasty for functional tricuspid regurgitation: two different patterns of right heart reverse remodelling. *Interact Cardiovasc Thorac Surg.* 2016;23:79-89.
32. Bothe W, Rausch MK, Kvitting JPE, Echnner DK, Walther M, Ingels NB, et al. How do annuloplasty rings affect mitral annular strains in the normal beating ovine heart? *Circulation.* 2012;126(11 Suppl 1):S213-38.
33. Navia JL, Nowicki ER, Blackstone EH, Brozzi NA, Nento DE, Atik FA, et al. Surgical management of secondary tricuspid valve regurgitation: annulus, commissure, or leaflet procedure? *J Thorac Cardiovasc Surg.* 2010;139:1473-82.e5.
34. Jazwiec T, Malinowski M, Proudfoot AG, Eberhart L, Langholz D, Schubert H, et al. Tricuspid valvular dynamics and 3-dimensional geometry in awake and anesthetized sheep. *J Thorac Cardiovasc Surg.* 2018;156:1503-11.

**Key Words:** tricuspid annulus, annuloplasty, strain

## Discussion



**Dr Song Wan** (*Hong Kong, China*). Congratulations, Dr Malinowski, for this excellent presentation, and I think this elegantly designed and carefully conducted study definitely will enhance our understanding about tricuspid valve geometry and dynamics.

My first question to you: Because your studies were all performed in healthy normal animals, one may assume the normal saddle shape of the tricuspid valve is well maintained before surgery. So it's a little bit surprising to see after flexible band annuloplasty basically it has completely flattened the tricuspid valve. And this is actually in contrast to our previous many experimental and clinical observations on the mitral valve, where the flexible band can maintain the saddle shape. So can you enlighten us a little bit on this aspect?



**Dr Marcin Malinowski** (*Grand Rapids, Mich*). Thank you so much for the question. Let me first address your first comment. Of course, this kind of a study had a certain limitation. It was done on healthy animals without previous annular dilation or previous functional tricuspid regurgitation. So

bearing it in mind, of course, we have to have limited extrapolation to the clinic. But, of course, as you correctly pointed out, that's what we saw, that implantation of that flexible band flattened the annulus. And we were surprised by that based on the decades of previous experiments on the mitral valve when, as you mentioned, the flexible rings

maintained the saddle shape.

I think that there may be a 2-fold explanation for this. First of all, we are on the right side, so we have completely different compliance of the right ventricle in comparison to the left side. And second, usually with this kind of study done previously on animals on the mitral side, we usually implanted the ring—the full ring—and here on the tricuspid side we used a band. So that may be another possible explanation.

But of course this is a very interesting finding and we would like to explore it more in the future.

**Dr Wan.** Okay. My second question—and, really, I appreciate you sharing your manuscript a few days early so that I can look into many details—you said you measured annular height to commissural width ratio at the maximal valve area time. If I understand correctly, that's the end-diastolic phase.

**Dr Malinowski.** That's around end-diastolic, because it differs animal to animal and not precisely at that time. But it was within the boundaries of the end-diastolic, that's correct.

**Dr Wan.** But the point is what we are really interested in is the end-systolic phase. We want to know the annular height to commissural width ratio at the end-systolic phase. That actually, again based on the mitral research, really matters.

**Dr Malinowski.** We have the data, so we will be glad to provide the data on any time point, basically.

**Dr Wan.** Excellent. Finally, a very short question. Any animal after weaning from cardiopulmonary bypass needed pacing, especially in the Contour 3D (Medtronic, Minneapolis, Minn) group?

**Dr Malinowski.** I think among 10 of them, 2 required pacing because of the way they are implanted, so that they cover most part of the septal leaflet, and in fact 2 required pacing, that's correct.

**Dr Wan.** I am not familiar with the animal conduction system anatomy, but based on our clinical experience, the TriAd Adams ring (Medtronic) can significantly avoid injury to the conduction system.

**Dr Malinowski.** The construction of the TriAd Adams ring is completely different. It's wide open, so that was the idea behind this design, to make it open to avoid this kind of conflict with the conduction system. And that's correct; we didn't see any conduction system interference with the other groups in contrast to the Contour 3D ring.

**Dr Wan.** Thank you, and once again, thanks for the honor of discussing this.

TABLE E1. Multiple comparisons for group characteristics\*

	Control (n = 10)	Duran AnCore (n = 10)	Contour 3D (n = 10)	TriAd Adams (n = 10)	P value†
Animal weight (kg)	53 ± 5	63 ± 4	66 ± 5	56 ± 4	<.001
		P value from multiple comparisons			
Control	–	.001	<.001	.262	
Duran AnCore	–	–	.262	.018	
Contour 3D	–	–	–	<.001	
Ring size (mm)	–	29 (2-29)	30 (28-30)	28 (26-28.5)	.017
		P value from multiple comparisons			
Control	–	–	–	–	
Duran AnCore	–	–	.083	>.999	
Contour 3D	–	–	–	.022	
CPB time (min)	79 ± 6	107 ± 11	118 ± 20	87 ± 11	<.001
		P value from multiple comparisons			
Control	–	<.001	<.001	.160	
Duran AnCore	–	–	.078	.003	
Contour 3D	–	–	–	<.001	
LVP max (mm Hg)	89 (81-91)	100 (94-104)	100 (95-110)	95 (82-98)	.005
		P value from multiple comparisons			
Control	–	.023	.016	>.999	
Duran AnCore	–	–	>.999	.415	
Contour 3D	–	–	–	.320	
RV EDV <sub>ind</sub> (mL)	77 ± 13	55 ± 13	71 ± 9	58 ± 15	.003
		P value from multiple comparisons			
Control	–	.008	.641	.024	
Duran AnCore	–	–	.061	.641	
Contour 3D	–	–	–	.130	

Values are presented as mean ± standard deviation or median (interquartile range [25th-75th percentile]). CPB, Cardiopulmonary bypass; LVP, left ventricular pressure; RV, right ventricle; EDV<sub>ind</sub>, indexed end diastolic volume. \*Duran AnCore, Contour 3D, and TriAd Adams (Medtronic, Mi, Minn). †P values from analysis of variance or analysis of variance on ranks. Each P value from post hoc analysis was adjusted for multiple comparisons.

TABLE E2. Multiple comparisons for tricuspid annular geometry, global dynamics, and strain, by ring type\*

Variable	Control (n = 10)	Duran AnCore (n = 10)	Contour3D (n = 10)	TriAd Adams (n = 10)	P value†
Maximal annular area (mm <sup>2</sup> )	967 ± 142	441 ± 61	408 ± 46	476 ± 83	<.001
	P value from multiple comparisons				
Control	–	<.001	<.001	<.001	
Duran AnCore	–	–	.630	.630	
Contour 3D	–	–	–	.271	
Minimal annular area (mm <sup>2</sup> )	880 ± 146	403 ± 55	401 ± 46	434 ± 89	<.001
	P value from multiple comparisons				
Control	–	<.001	<.001	<.001	
Duran AnCore	–	–	.952	.753	
Contour 3D	–	–	–	.753	
Annular contraction (%)	10 (9-12)	8 (7-11)	2 (1-2)	7 (6-12)	<.001
	P value from multiple comparisons				
Control	–	>.999	<.001	.841	
Duran AnCore	–	–	.002	>.999	
Contour 3D	–	–	–	.007	
Maximal annular height (mm)	6.2 ± 2.0	3.1 ± 1.3	4.9 ± 1.1	3.1 ± 1.0	<.001
	P value from multiple comparisons				
Control	–	<.001	.130	<.001	
Duran AnCore	–	–	.024	.994	
Contour 3D	–	–	–	.024	
Annular height change (%)	23 ± 16	21 ± 13	7 ± 3	22 ± 14	.021
	P value from multiple comparisons				
Control	–	.962	.037	.968	
Duran AnCore	–	–	.072	.968	
Contour 3D	–	–	–	.052	
AHCWR diastole (%)	17 ± 6	11 ± 6	19 ± 4	10 ± 4	<.001
	P value from multiple comparisons				
Control	–	.028	.759	.011	
Duran AnCore	–	–	.008	.759	
Contour 3D	–	–	–	.002	
AHCWR systole (%)	16 ± 7	11 ± 5	20 ± 4	10 ± 3	<.001
	P value from multiple comparisons				
Control	–	.115	.160	.076	
Duran AnCore	–	–	.002	.755	
Contour 3D	–	–	–	<.001	
Global annular strain (%)	–5.3 ± 1.8	–2.3 ± 1.0	–0.6 ± 0.2	–2.6 ± 0.7	<.001
	P value from multiple comparisons				
Control	–	<.001	<.001	<.001	
Duran AnCore	–	–	.003	.442	
Contour 3D	–	–	–	<.001	

Values are presented as mean ± standard deviation or median (interquartile range [25th-75th percentiles]). AHCWR, Annular to commissural width ratio. \*Duran AnCore, Contour 3D, and TriAd Adams (Medtronic, Minneapolis, Minn). †P values from analysis of variance or analysis of variance on ranks. Each P value from post hoc analysis was adjusted for multiple comparisons.

TABLE E3. Multiple comparisons for tricuspid annular diameters, based on ring tested\*

	Control (n = 10)	Duran AnCore (n = 10)	Contour 3D (n = 10)	TriAd Adams (n = 10)	P value†
<b>S-L diameter</b>					
Maximal (mm)	33.6 (32.0-35.4)	19.8 (18.5-23.4)	19.0 (18.2-21.2)	20.6 (18.8-21.7)	<.001
	<i>P</i> value from multiple comparisons				
Control	–	.002	<.001	.003	
Duran AnCore	–	–	>.999	>.999	
Contour 3D	–	–	–	>.999	
Minimal (mm)	31.0 ± 2.0	19.7 ± 3.0	19.4 ± 2.4	20.1 ± 3.2	<.001
	<i>P</i> value from multiple comparisons				
Control	–	<.001	<.001	<.001	
Duran AnCore	–	–	.934	.934	
Contour 3D	–	–	–	.908	
Shortening (%)	5.3 (4.4-13.7)	5.9 (4.8-6.9)	1.0 (0.5-1.3)	3.9 (3.2-5.4)	<.001
	<i>P</i> value from multiple comparisons				
Control	–	>.999	<.001	.785	
Duran AnCore	–	–	<.001	>.999	
Contour 3D	–	–	–	.023	
<b>A-P diameter</b>					
Maximal (mm)	36.7 ± 2.6	22.7 ± 2.3	24.6 ± 1.7	27.8 ± 3.3	<.001
	<i>P</i> value from multiple comparisons				
Control	–	<.001	<.001	<.001	
Duran AnCore	–	–	.189	<.001	
Contour 3D	–	–	–	.016	
Minimal (mm)	33.8 ± 3.7	22.3 ± 2.4	24.5 ± 1.7	26.6 ± 3.5	<.001
	<i>P</i> value from multiple comparisons				
Control	–	<.001	<.001	<.001	
Duran AnCore	–	–	.223	.009	
Contour 3D	–	–	–	.223	
Shortening (%)	10.1 (3.0-12.9)	2.6 (2.0-3.4)	0.4 (0.2-0.8)	4.4 (2.0-6.1)	<.001
	<i>P</i> value from multiple comparisons				
Control	–	.193	<.001	>.999	
Duran	–	–	.030	>.999	
Contour	–	–	–	.001	
<b>C-C 1-3</b>					
Maximal (mm)	29.5 ± 2.8	16.4 ± 2.2	21.5 ± 1.6	21.3 ± 2.3	<.001
	<i>P</i> value from multiple comparisons				
Control	–	<.001	<.001	<.001	
Duran AnCore	–	–	<.001	<.001	
Contour 3D	–	–	–	.904	
Minimal (mm)	26.7 ± 2.3	16.2 ± 2.2	21.3 ± 1.6	19.7 ± 2.2	<.001
	<i>P</i> value from multiple comparisons				
Control	–	<.001	<.001	<.001	
Duran AnCore	–	–	<.001	<.001	
Contour 3D	–	–	–	.089	
Shortening (%)	8.8 (5.9-13.9)	1.5 (0.7-2.3)	0.6 (0.4-0.8)	6.3 (4.3-11.9)	<.001
	<i>P</i> value from multiple comparisons				
Control	–	.003	<.001	>.999	
Duran AnCore	–	–	>.999	.021	
Contour 3D	–	–	–	<.001	

(Continued)

ADULT

TABLE E3. Continued

	Control (n = 10)	Duran AnCore (n = 10)	Contour 3D (n = 10)	TriAd Adams (n = 10)	P value†
<b>C-C 3-5</b>					
Maximal (mm)	32.4 (22.3-41.8)	17.9 (16.3-19.9)	13.6 (12.3-18.8)	20.4 (16.6-22.7)	<.001
	<i>P</i> value from multiple comparisons				
Control	–	.018	<.001	.101	
Duran AnCore	–	–	.268	>.999	
Contour 3D	–	–	–	.059	
Minimal (mm)	30.8 (21.5-40.7)	17.7 (16.2-19.7)	13.5 (12.2-16.7)	20.1 (16.2-22.5)	<.001
	<i>P</i> value from multiple comparisons				
Control	–	.016	<.001	.118	
Duran AnCore	–	–	.335	>.999	
Contour 3D	–	–	–	.059	
Shortening (%)	3.7 ± 1.1	1.7 ± 1.0	0.6 ± 0.4	1.2 ± 0.7	<.001
	<i>P</i> value from multiple comparisons				
Control	–	<.001	<.001	<.001	
Duran AnCore	–	–	.026	.294	
Contour 3D	–	–	–	.184	
<b>C-C 5-1</b>					
Maximal (mm)	40.8 ± 5.4	26.8 ± 2.4	23.1 ± 2.3	27.9 ± 2.6	<.001
	<i>P</i> value from multiple comparisons				
Control	–	<.001	<.001	<.001	
Duran AnCore	–	–	.046	.485	
Contour 3D	–	–	–	.012	
Minimal (mm)	37.5 ± 5.3	25.9 ± 2.5	22.9 ± 2.3	26.9 ± 2.7	<.001
	<i>P</i> value from multiple comparisons				
Control	–	<.001	<.001	<.001	
Duran AnCore	–	–	.119	.525	
Contour 3D	–	–	–	.043	
Shortening (%)	7.3 (5.3-11.9)	2.9 (2.3-3.5)	0.6 (0.4-1.1)	3.0 (2.0-4.9)	<.001
	<i>P</i> value from multiple comparisons				
Control	–	.452	<.001	.532	
Duran AnCore	–	–	.016	>.999	
Contour 3D	–	–	–	.012	

Values are presented as mean ± standard deviation or median (interquartile range [25th-75th percentile]). Crystal numbers for C-C distances as depicted in Figure 1: Crystal #1, anteroseptal commissure; crystal #3, anteroposterior commissure; crystal #5, posteroseptal commissure. *S-L*, Septo-lateral; *A-P*, antero-posterior; *C-C*, intercommissural distances. \*Duran AnCore, Contour 3D, and TriAd Adams (Medtronic, Minneapolis, Minn). †*P* values from analysis of variance or analysis of variance on ranks. Each *P* value from post hoc analysis was adjusted for multiple comparisons.



TABLE E4. Multiple comparisons for regional tricuspid annular dynamic parameters of rings tested\*

Parameter	Ring	Control (n = 10)	Duran AnCore (n = 10)	Contour 3D (n = 10)	TriAd Adams (n = 10)	P value†
Anterior contraction (%)	Overall	6.6 (4.4-10.9)	1.1 (0.6-1.9)	0.98 (0.6-1.1)	6.4 (5.4-8.5)	<.001
		<i>P</i> value from multiple comparisons				
	Control	–	.002	<.001	>.999	
	Duran AnCore	–	–	>.999	.005	
	Contour 3D	–	–	–	<.001	
	1-2 (%)	11.8 (5.3-16.1)	2.0 (1.4-2.5)	1.2 (0.7-1.6)	13.8 (10.1-16.0)	<.001
		<i>P</i> value from multiple comparisons				
	Control	–	.049	<.001	>.999	
	Duran AnCore	–	–	>.999	.006	
	Contour 3D	–	–	–	<.001	
	2-3 (%)	12.0 (5.9-14.2)	2.2 (1.6-3.4)	1.4 (1.1-2.2)	1.8 (1.4-2.4)	<.001
	Control	–	.015	<.001	.013	
Duran AnCore	–	–	.112	>.999		
Contour 3D	–	–	–	.817		
Posterior contraction (%)	Overall	5.0 (3.5-7.9)	1.9 (1.1-2.6)	0.9 (0.6-0.9)	1.4 (0.9-2.1)	<.001
		<i>P</i> value from multiple comparisons				
	Control	–	.05	<.001	.007	
	Duran AnCore	–	–	.082	>.999	
	Contour 3D	–	–	–	.381	
	3-4 (%)	5.8 (4.1-7.9)	3.0 (2.4-3.5)	1.2 (0.9-1.6)	1.8 (1.4-2.4)	<.001
		<i>P</i> value from multiple comparisons				
	Control	–	.124	<.001	.003	
	Duran AnCore	–	–	.033	>.999	
	Contour 3D	–	–	–	.624	
	4-5 (%)	9.4 (3.9-13.2)	2.3 (2.0-3.4)	2.0 (1.8-2.2)	2.9 (2.2-4.3)	<.001
		<i>P</i> value from multiple comparisons				
Control	–	.015	<.001	.101		
Duran AnCore	–	–	.880	>.999		
Contour 3D	–	–	–	.215		
Septal contraction (%)	Overall	11.9 ± 5.4	10.2 ± 3.9	1.7 ± 0.6	7.7 ± 2.8	<.001
		<i>P</i> value from multiple comparisons				
	Control	–	.291	<.001	.043	
	Duran AnCore	–	–	<.001	.248	
	Contour 3D	–	–	–	.002	
	5-6 (%)	11.0 (8.7-17.2)	12.9 (6.4-18.7)	2.0 (1.8-2.2)	8.9 (6.8-12.1)	<.001
		<i>P</i> value from multiple comparisons				
	Control	–	>.999	<.001	>.999	
	Duran AnCore	–	–	<.001	>.999	
	Contour 3D	–	–	–	.012	
	6-1 (%)	4.8 (2.3-9.3)	6.4 (4.1-8.3)	1.6 (1.1-2.1)	5.8 (3.9-7.7)	.002
		<i>P</i> value from multiple comparisons				
Control	–	>.999	.015	>.999		
Duran AnCore	–	–	.005	>.999		
Contour 3D	–	–	–	.011		

Values are presented as mean ± standard deviation or median (interquartile range [25th-75th percentiles]). Regional annular contraction was calculated based on regional annular length change throughout the cardiac cycle. Crystal numbers as depicted in Figure 1. Anterior annulus crystals #1, 2, 3; posterior annulus crystals #3, 4, 5; septal annulus crystals #5, 6, 1; crystal #1, anteroseptal commissure; crystal #3, anteroposterior commissure; crystal #5, posteroseptal commissure. \*Duran AnCore, Contour 3D, and TriAd Adams (Medtronic, Minneapolis, Minn). †*P* values from analysis of variance or analysis of variance on ranks. Each *P* value from post hoc analysis was adjusted for multiple comparisons.

ADULT